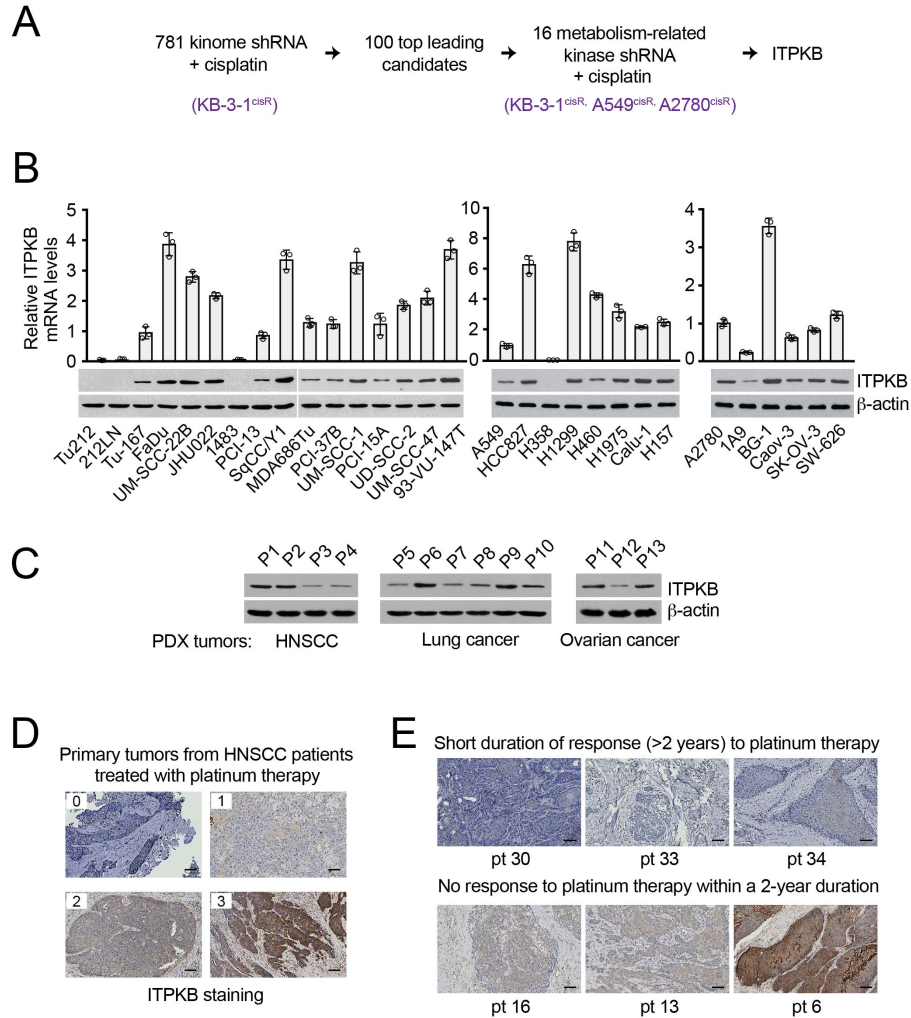


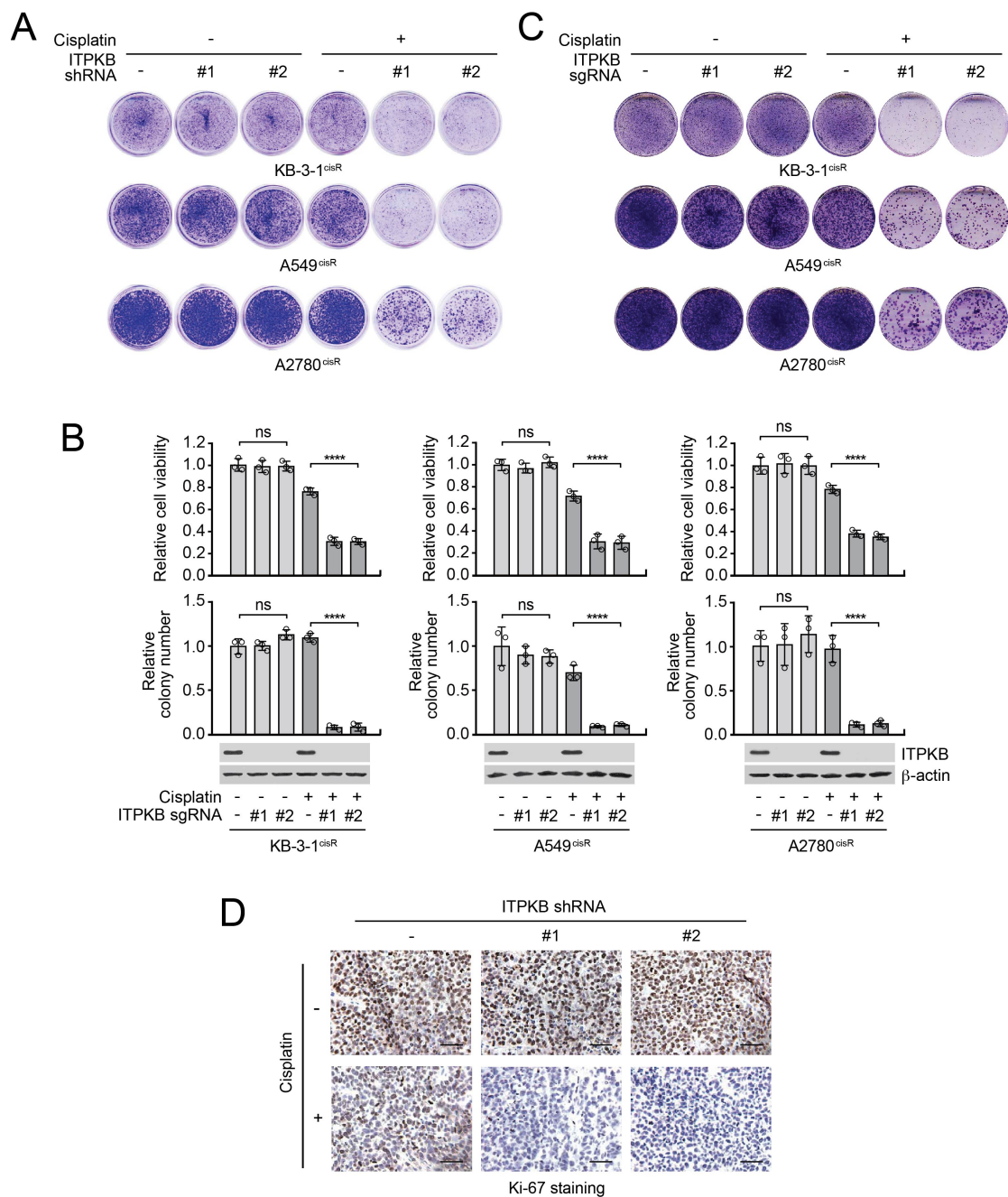
Inositol-triphosphate 3-kinase B confers cisplatin resistance by regulating NOX4-dependent redox balance

Pan et al.

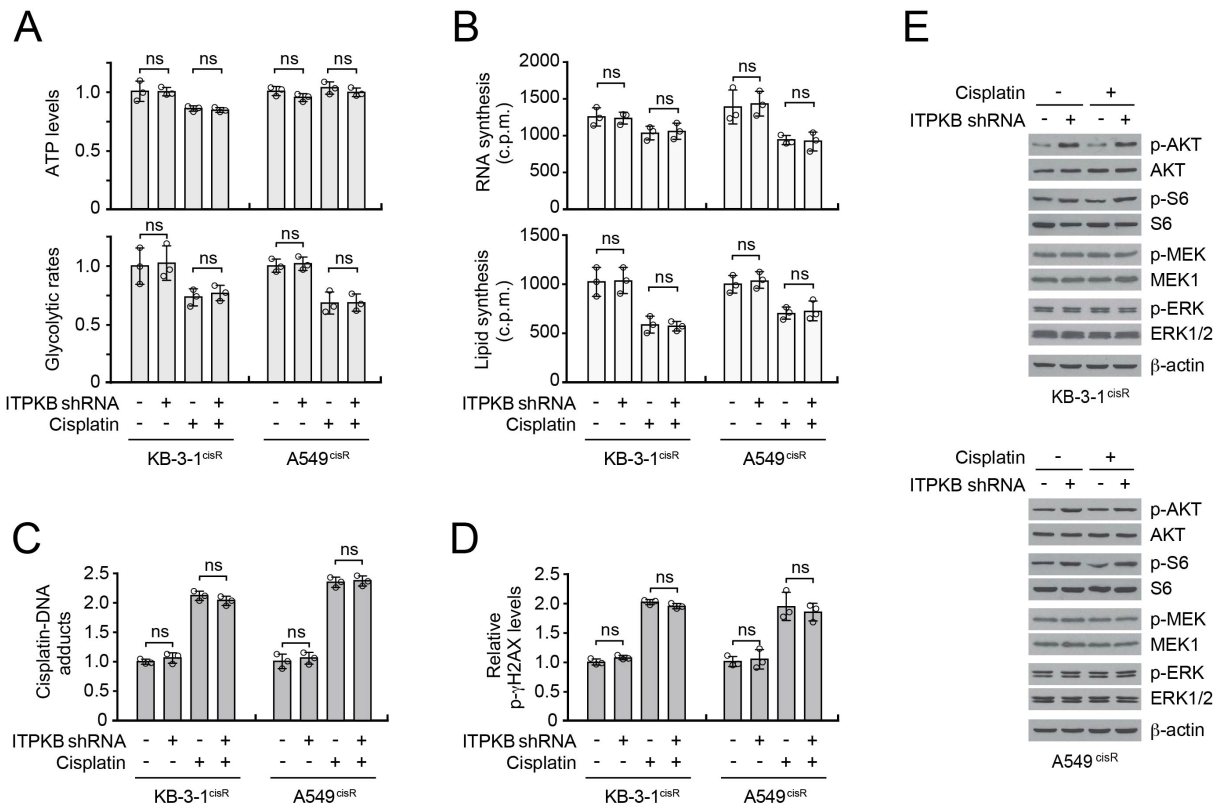
Supplemental Data



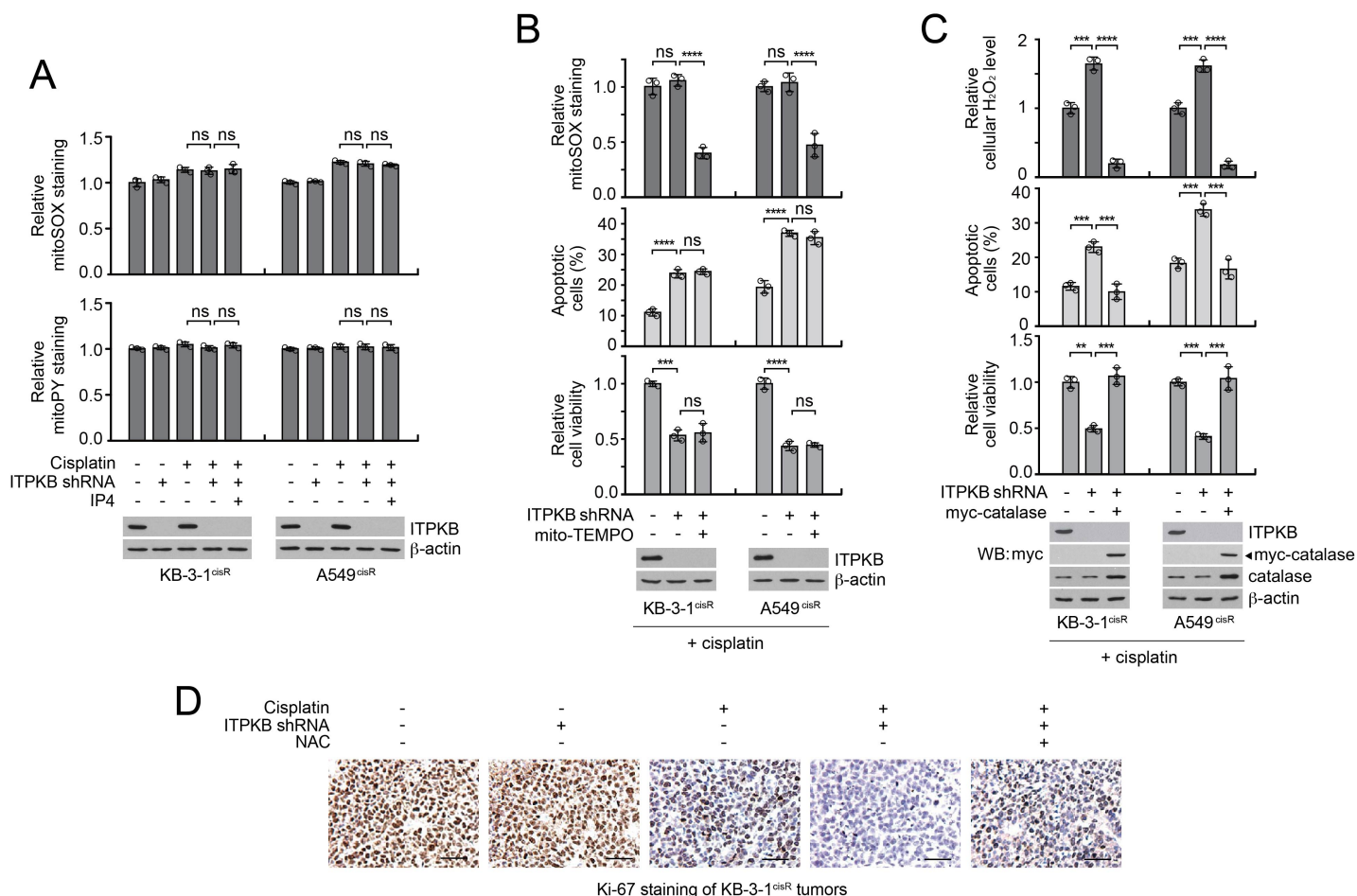
Supplemental Figure 1. ITPKB expression positively associated with cisplatin resistance in cancer cell lines and primary cancer patient samples. (A) Schematic view of RNAi screen. **(B)** The mRNA and protein level of ITPKB in a panel of cancer cell lines. **(C)** ITPKB expression levels in head and neck, lung, and ovarian cancer patient-derived xenograft (PDX) tumors. **(D)** Representative images of scores 0, 1, 2, 3 for ITPKB immunohistochemistry (IHC) staining using primary tumor specimens collected from head and neck squamous cell carcinoma (HNSCC) patients treated with platinum therapy are shown. **(E)** Representative ITPKB IHC images of tumors from HNSCC patient groups who showed response (*top*) or no response (*bottom*) to platinum therapy within a two-year duration are shown. Scale bars represent 100 μm. Data are mean ± SD of three technical replicates (B *top*) and are representative two (B, C) independent biological experiments.



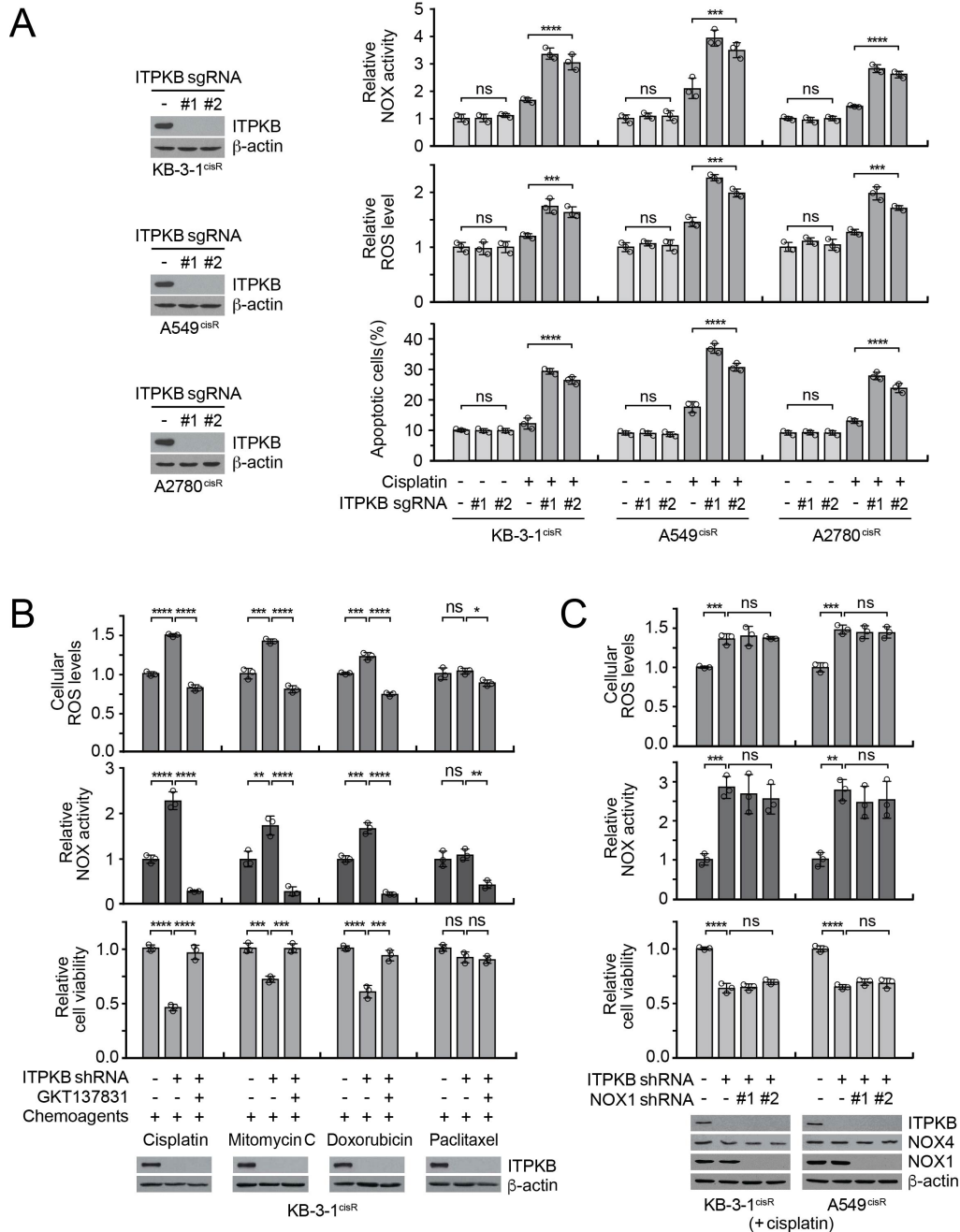
Supplemental Figure 2. Knockdown or knockout of ITPKB attenuates cisplatin-resistant cancer cell proliferation. (A) Representative images of colony formation assays using ITPKB knockdown cells are shown. (B) Cell viability (*top*) and colony formation potential (*bottom*) of KB-3-1^{cisR}, A549^{cisR}, and A2780^{cisR} cells with ITPKB knockout in the presence or absence of cisplatin. Cells were transduced with ITPKB sgRNA clones and treated with sub-lethal doses of cisplatin (KB-3-1^{cisR} and A2780^{cisR} 5 μ g/ml, A549^{cisR}: 2 μ g/ml) for 48 hr for cell viability. ITPKB knockout efficiency was assessed by immunoblotting. (C) Representative images of colony formation assays using ITPKB knockout cells are shown. (D) Proliferation rates of KB-3-1^{cisR} xenograft tumors from Figure 2C were assessed by Ki-67 staining. Scale bars represent 50 μ m for Ki-67 staining. Data are mean \pm SD from three technical replicates of each sample and are representative of three (B; top) and one (B; middle) independent biological experiments. Statistical analysis was performed by 1-way ANOVA (ns: not significant; **** $P < 0.0001$).



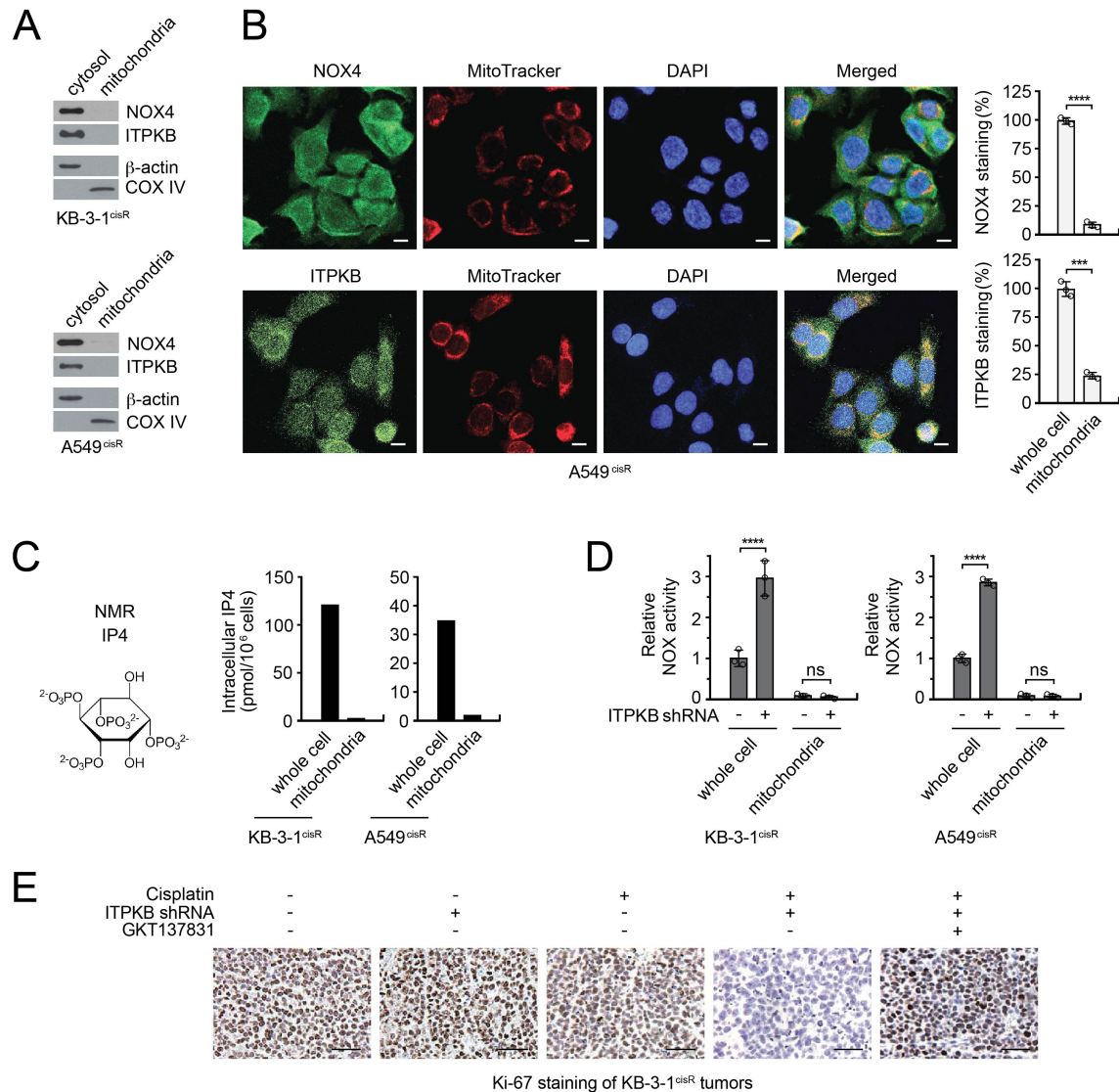
Supplemental Figure 3. Knockdown of ITPKB and cisplatin treatment neither affect bioenergetics and anabolic biosynthesis nor attenuate activity of AKT and MEK. (A and B) Effect of ITPKB knockdown and cisplatin treatment on bioenergetics (A), RNA and lipid biosynthesis (B). Cells were treated with sub-lethal doses of cisplatin (KB-3-1^{cisR}: 5 μg/ml, A549^{cisR}: 2 μg/ml). ATP levels and glycolytic rates were measured to profile bioenergetics. RNA and lipid synthesis levels were determined by measuring ¹⁴C incorporation in RNA or lipid from ¹⁴C-glucose in cells. **(C and D)** Effect of targeting ITPKB on cisplatin uptake (C) and cisplatin-induced DNA damage (D) in cells with ITPKB knockdown and cisplatin treatment as in (A), were quantified using specific antibodies against cisplatin-DNA adducts and phospho-γH2AX, respectively. **(E)** Targeting ITPKB activates AKT but not MEK, and cisplatin treatment together with ITPKB knockdown does not further alter the AKT or MAPK pathway. Cells were treated with cisplatin as in (A) and activation of the AKT pathway was examined by assessing phosphorylation levels of AKT (T308) and S6 (S240/S244). Activation of MAPK pathway was assessed by phospho-MEK (S221) and phospho-ERK1/2(T202/Y204). Data are mean ± SD from three technical replicates of each sample and are representative of two independent biological experiments. Statistical analysis was performed by 1-way ANOVA (ns: not significant).



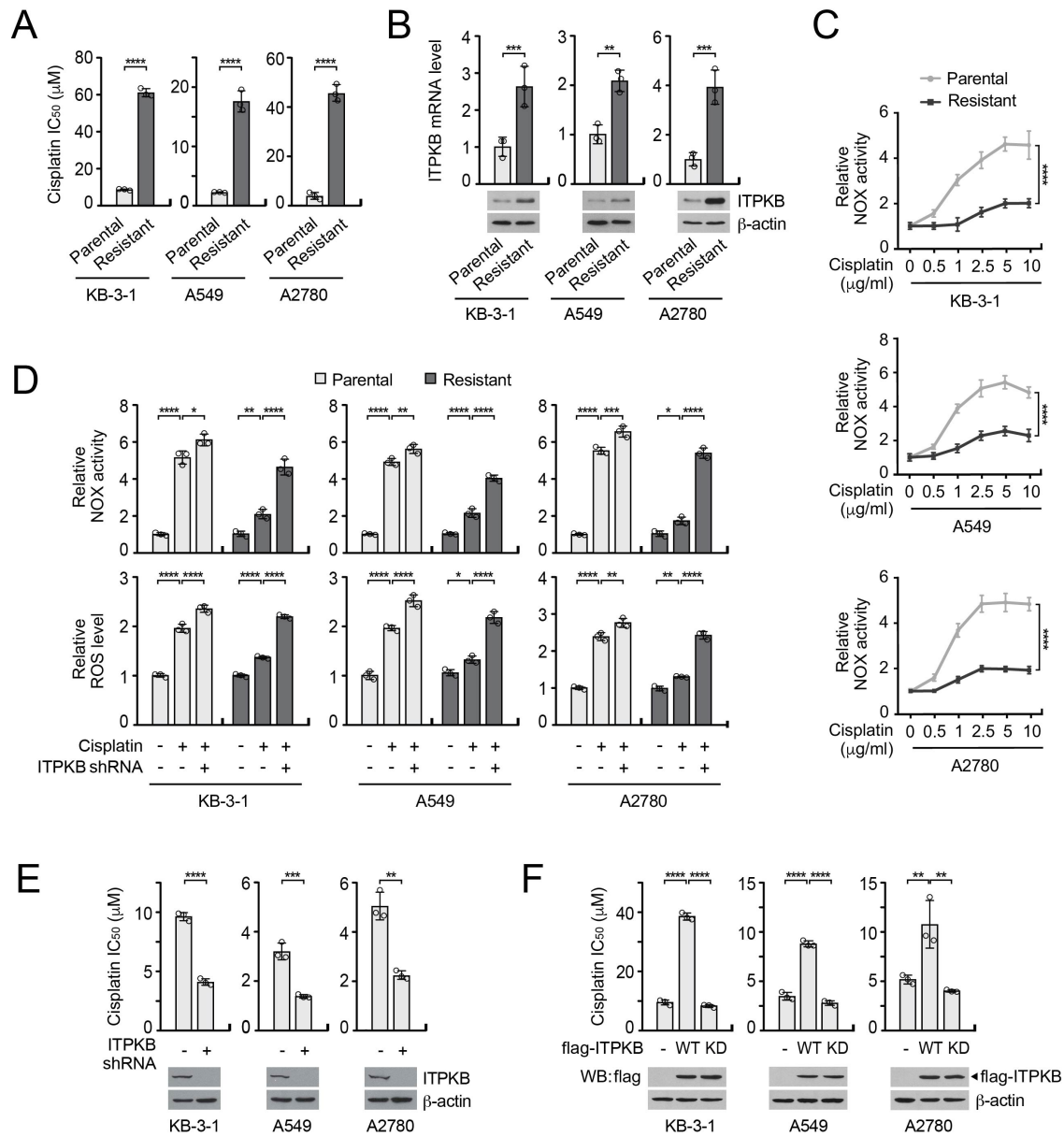
Supplemental Figure 4. ITPKB contributes to cisplatin-resistant cell survival by controlling cytosolic ROS but not mitochondrial ROS. (A) Effect of ITPKB knockdown and extracellular IP4 on cisplatin-induced mitochondrial ROS. Cells were incubated with 1 μ M IP4-PM and sublethal doses of cisplatin ((KB-3-1^{cisR}: 5 μ g/ml, A549^{cisR}: 2 μ g/ml). Mitochondrial superoxide and mitochondrial H₂O₂ were determined using mitoSOX and mitoPY1, respectively. **(B-C)** Effect of mito-TEMPO (B) or catalase overexpression (C) on ROS, apoptosis, and cell viability in cells with ITPKB knockdown and cisplatin treatment. 10 μ M of mito-TEMPO or myc tagged catalase were introduced in cisplatin treated cells as in (A). Apoptotic cell death and cell viability were assessed by annexin V staining and CellTiter-Glo Luminescent Viability Assay. **(D)** Representative images of Ki-67 IHC staining in harvested tumors from each group of KB-3-1^{cisR} xenograft mice from Figure 5D are shown. Scale bars represent 50 μ m. Data are mean \pm SD from three technical replicates of each sample and are representative of three independent biological experiments. Statistical analysis was performed by 1-way ANOVA (ns: not significant; ** P < 0.01; *** P < 0.005; **** P < 0.0001).



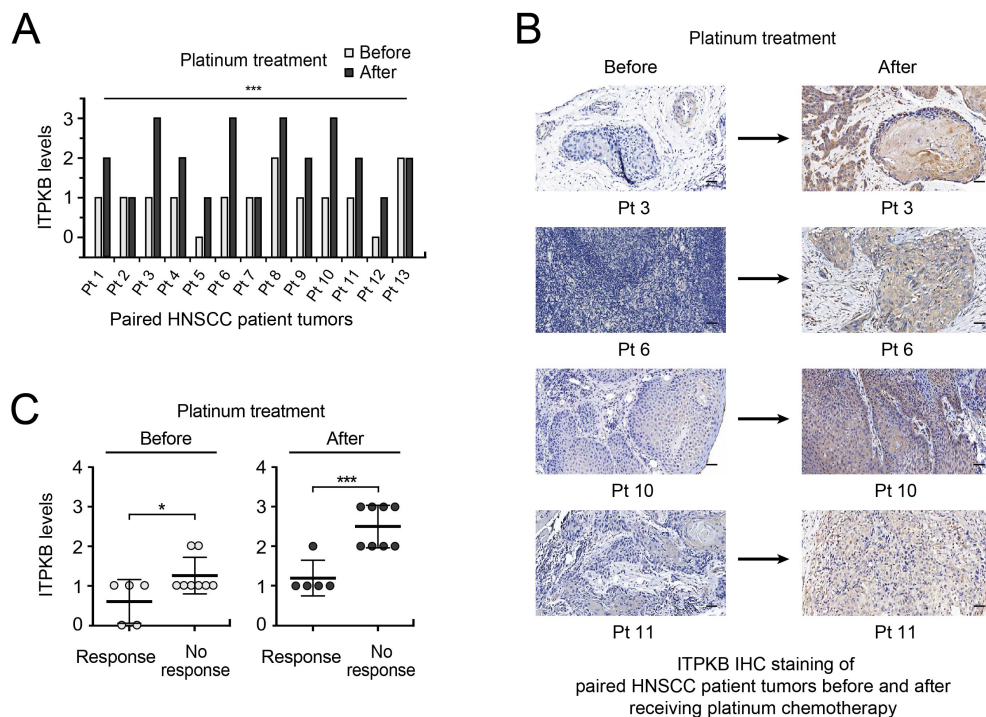
Supplemental Figure 5. ITPKB confers resistance to DNA damaging agents by inhibiting NOX4 activity in cancer cells. (A) Effect of ITPKB knockout on NOX activity, ROS level, and apoptosis in the presence and absence of cisplatin. **(B)** Effect of NOX inhibitor GKT137831 on ROS level, NOX activity, and cell viability in ITPKB knockdown cells in the presence of paclitaxel or DNA damaging agents. KB-3-1^{cisR} cells were treated with sublethal doses of chemotherapy agents (5 μ g/ml cisplatin, 0.2 μ M doxorubicin, 2 μ M mitomycin C, 1 nM paclitaxel) and GKT137831 (10 μ M). ROS/NOX activity and cell viability were determined after 12 hr and 48 hr, respectively. **(C)** Effect of NOX1 knockdown on ROS level, NOX activity, and cell viability in ITPKB knockdown cells in the presence of cisplatin. Data are mean \pm SD from three technical replicates of each sample and are representative of two independent biological experiments. Statistical analysis was performed by 1-way ANOVA (ns: not significant; * P < 0.05; ** P < 0.01; *** P < 0.005; **** P < 0.0001).



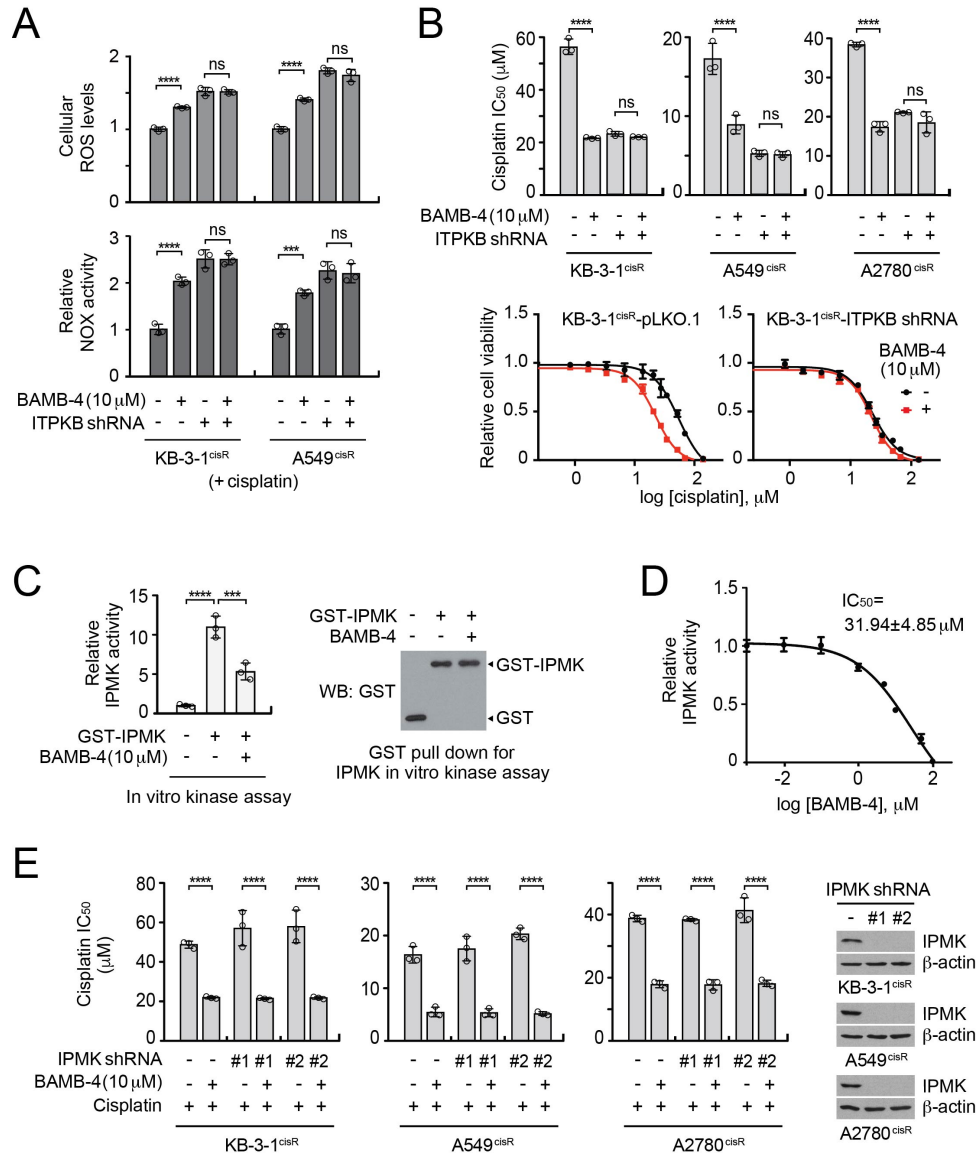
Supplemental Figure 6. NOX4, ITPKB, and IP4 predominantly localize in the cytosol and ITPKB inhibit NOX in the cytosol to confer cisplatin-resistant tumor growth. (A) Subcellular localization of NOX4 and ITPKB. β -actin and COX IV were used as control markers for cytosol and mitochondria, respectively. Cytosolic and mitochondrial fractions were prepared from KB-3-1^{cisR} and A549^{cisR} cells using mitochondria isolation kit. (B) Immunofluorescence assay of NOX4 and ITPKB. Mitochondria and nucleus were stained with mitochondrial marker MitoTracker and DAPI, respectively. Scale bars = 10 μ m. (C) Amount of IP4 in total cell and mitochondria was obtained by ³¹P nuclear magnetic resonance (NMR) spectroscopy. Concentrations in cells are shown as pmol/10⁶ cells. (D) NOX activity in whole cell and mitochondria fraction of KB-3-1^{cisR} and A549^{cisR} cells with ITPKB knockdown and cisplatin treatment. (E) Representative images of Ki-67 IHC staining in harvested tumors from each group of KB-3-1^{cisR} xenograft mice from Figure 6F are shown. Scale bars represent 50 μ m. Data are mean \pm SD from three technical replicates. Data shown are representative of two (A and B), one (C), and three (D) independent biological experiments. Statistical analysis was performed by two-tailed Student's *t* test for (B) and 1-way ANOVA for (D) (ns: not significant; ****P* < 0.005; *****P* < 0.0001).



Supplemental Figure 7. ITPKB contributes to cisplatin resistance in both parental and cisplatin-resistant cancer cells. (A-C) Three pairs of parental and cisplatin-resistant cells were compared for cisplatin IC₅₀ (A), ITPKB RNA level (B), and NOX activity upon cisplatin exposure (C). (D) Effect of ITPKB knockdown on NOX activity and ROS level in pairs of parental and cisplatin-resistant cell lines. (E-F) Effect of ITPKB knockdown (E) or wild type or kinase-dead mutant ITPKB D897N overexpression (F) on cisplatin response in diverse parental cancer cell lines. Data are mean ± SD from three technical replicates and are representative of three (A-D) and two (E and F) independent biological experiments. Statistical analysis was performed by two-tailed Student's *t* test for (A, B, E), 2-way ANOVA for (C), and 1-way ANOVA for (D) and (F) (ns: not significant; **P* < 0.05; ***P* < 0.01; ****P* < 0.005; *****P* < 0.0001).

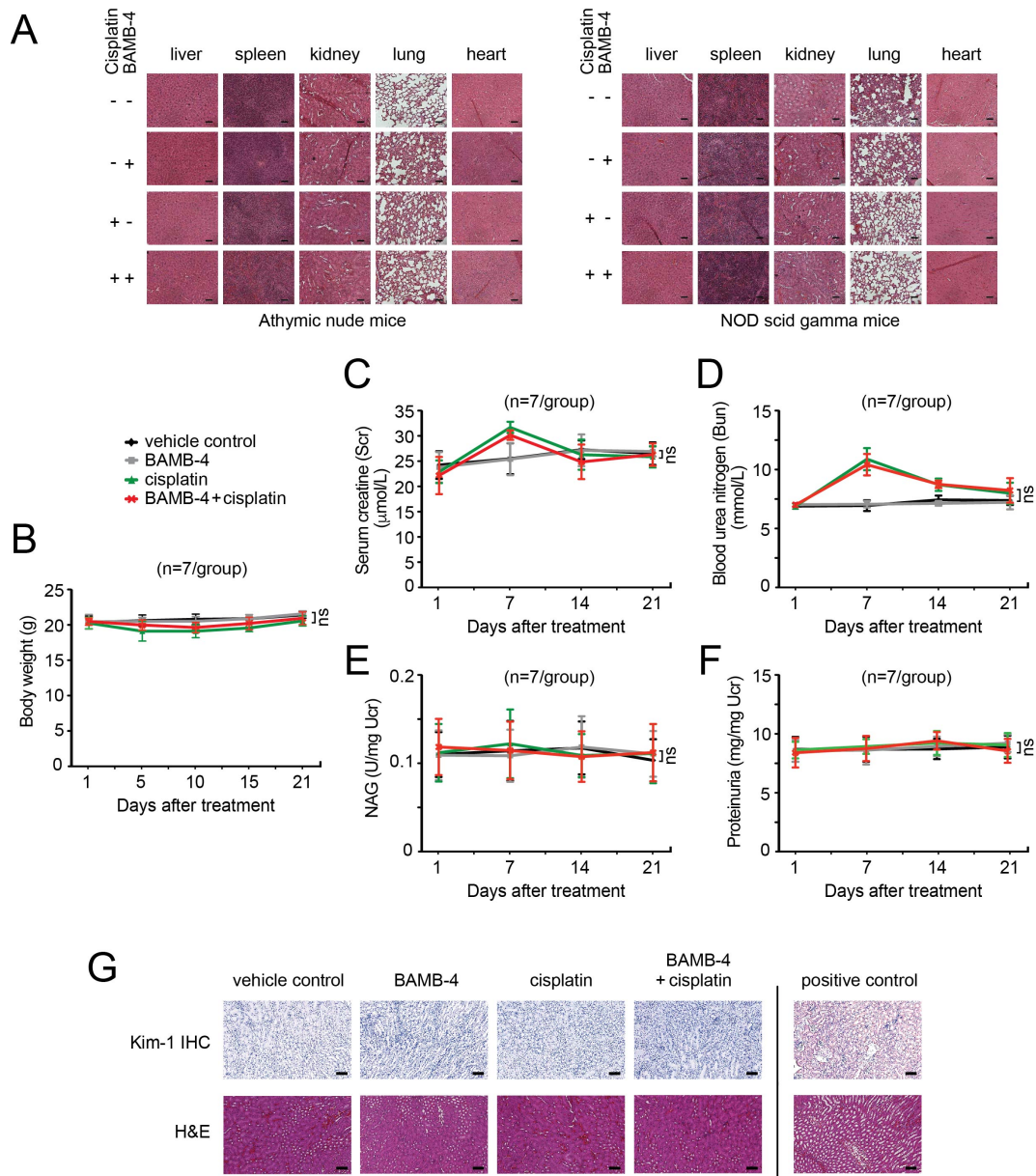


Supplemental Figure 8. ITPKB expression is more abundant in HNSCC patient tumors collected after platinum therapy compared to the paired tumors collected before treatment. (A) ITPKB expression in paired primary HNSCC patient tumors. **(B)** Representative tumor pairs are shown. Scale bars represent 100 μ m. **(C)** Comparison of ITPKB staining intensity between HNSCC patient groups who showed response or no response to platinum therapy within a two-year duration. Tumors were collected before or after platinum therapy. Response: patients who responded to platinum therapy for a duration of two years; No response: patients who lost response within the two-year period and had regrowth of tumors off treatment. Data are mean \pm SD from n=5 for 'Response' group and n=8 for 'No response' group. Statistical analysis was performed by paired two-tailed Student's *t* test for (A) and non-paired two-tailed Student's *t* test for (C) (* P < 0.05; *** P < 0.005).

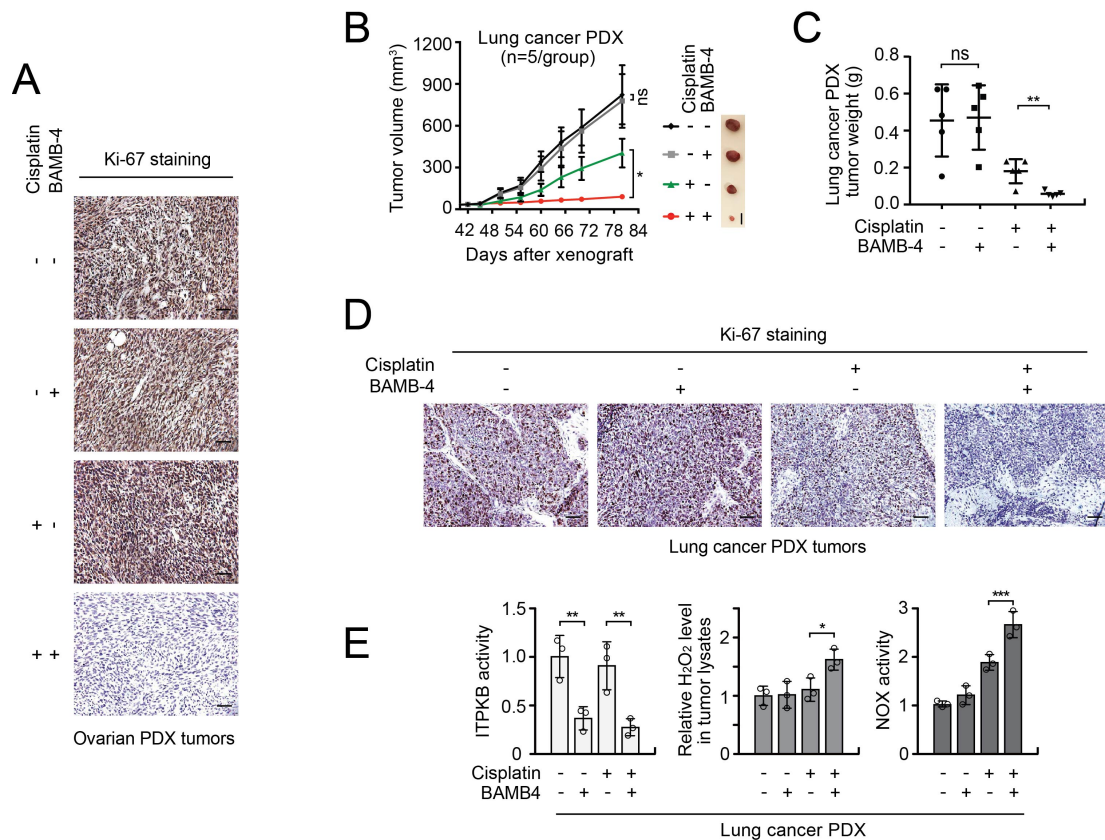


Supplemental Figure 9. BAMB-4 sensitizes cells to cisplatin by inhibiting ITPKB not IPMK.

(A) Effect of BAMB-4 on ROS level and NOX activity in cisplatin treated cells with or without ITPKB knockdown. Cells were treated with cisplatin (KB-3-1^{cisR}: 5 μg/ml, A549^{cisR}: 2 μg/ml) and BAMB-4 (10 μM) for 12 hr and ROS and NOX activity were examined. (B) Effect of BAMB-4 on cisplatin IC₅₀ in cells with or without ITPKB. (C) Effect of BAMB-4 on IPMK activity. GST-IPMK was enriched from cells by GST-pull down and IPMK activity was assessed by ADP-Glo kinase assay using IP3 as a substrate. (D) In vitro IPMK activity was measured in the presence of increasing concentrations of BAMB-4. (E) Effect of BAMB-4 on cisplatin response in cells with or without IPMK knockdown. Cells were treated with cisplatin (KB-3-1^{cisR} and A2780^{cisR}: 5 μg/ml, A549^{cisR}: 2 μg/ml) and BAMB-4 (10 μM) for 48 hr and cisplatin IC₅₀ was measured. Data are mean ± SD from three technical replicates and are representative of two independent biological experiments. Statistical analysis was performed by 1-way ANOVA (ns: not significant; ****P* < 0.005; *****P* < 0.0001).



Supplemental Figure 10. BAMB-4 and cisplatin induced no significant toxicity or kidney injury in mice. (A) Histology of hematoxylin and eosin (H&E) stained tissues of representative mice in vehicle control, cisplatin, BAMB-4, and combination treated groups. Athymic nude mice (lung cancer PDX) and NOD scid gamma mice (ovarian cancer PDX) were treated with 5 mg/kg of cisplatin and 10 mg/kg of BAMB-4 intraperitoneally twice a week for 38 days in nude mice and 16 days in NSG mice. Scale bars in (A) represent 50 μm . (B-G) Nephrotoxicity was assessed by measuring body weight (B) and quantification of kidney injury biomarkers including Scr (C), Bun (D), NAG activity (E), proteinuria (F), and kim-1 staining (G). 5 mg/kg of cisplatin and 10 mg/kg of BAMB-4 intraperitoneally twice a week for 21 days in nude mice for (B)-(G). Positive control group for kim-1 staining was administered 10 mg/kg/day of cisplatin for 3 consecutive days (n=7/group). Scale bars in (G) represent 100 μm . Data are mean \pm SD from 7 mice/group. Statistical analysis was performed by 2-way ANOVA (ns: not significant).



Supplemental Figure 11. Pharmacological inhibition of ITPKB sensitizes cancer cells to cisplatin treatment and attenuated tumor growth in ovarian and lung cancer PDX mice. (A) Representative Ki-67 staining images of tumors from each group of Figure 8C ovarian cancer PDX are shown. **(B and C)** Effect of BAMB-4 and/or cisplatin treatment on tumor growth (B) and tumor size (C) of lung cancer PDX mice. Mice were treated with cisplatin (5 mg/kg) and BAMB-4 (10 mg/kg) by i.p. injection twice a week from 42 days after xenograft. **(D)** Representative Ki-67 staining images of tumors from each group of lung cancer PDX are shown. **(E)** Effect of BAMB-4 and/or cisplatin treatment on ITPKB activity, H₂O₂ level, and NOX activity in lung cancer PDX tumors are shown. Scale bars represent 50 μ m for (A and D) and 10 mm for (B). Error bars represent SEM for (B) and SD for (C)(n=5). Data are mean \pm SD from three technical replicates of each sample and are representative of two independent biological experiments for (E). Statistical analysis was performed by 2-way ANOVA for (B) and 1-way ANOVA for all other data (ns: not significant; * $P < 0.05$; ** $P < 0.01$; *** $P < 0.005$).

	Sample #	Gender	Age	Diagnosis/subtype	Tumor stage	Treatment history	^a Time interval (months)	ITPKB staining
Figure 1D	1	F	67	HNSCC/Oropharynx	T4 N2c M0	Cisplatin	14	3
	2	M	65	HNSCC/Larynx	T2 N2b M0	Carboplatin, Paclitaxel	16	2
Sup Figure 1D-1E	3	M	51	HNSCC/Larynx	T2 N1 M0	Carboplatin, Paclitaxel	5	3
	4	M	60	HNSCC/Hypopharynx	T2 N2c M0	Cisplatin, Cetuximab	20	2
	5	M	72	HNSCC/Oropharynx	rT4a N0 M0	Carboplatin, Cetuximab	9	2
	6	M	61	HNSCC/Larynx	T4a N2b M0	Carboplatin	20	3
	7	M	53	HNSCC/Nasal Cavity	rT4a N0 M0	Cisplatin	2	3
	8	M	73	HNSCC/Hypopharynx	T4b N0 M0	Cisplatin	12	3
	9	M	62	HNSCC/Larynx	T4b N1 M0	Carboplatin	14	3
	10	M	71	HNSCC/Larynx	T1 N0 M0	Cisplatin or Carboplatin	6	1
	11	M	62	HNSCC/Larynx	T2 N0 M0	Cisplatin	10	3
	12	M	59	HNSCC/Larynx	T1 N0 M0	Carboplatin	5	1
	13	M	55	HNSCC/Larynx	T1 N0 M0	Cisplatin	7	2
	14	M	47	HNSCC/Larynx	T4 N2c M0	Cisplatin	7	3
	15	M	51	HNSCC/Larynx	rT4a N0 M0	Cisplatin	22	3
	16	M	72	HNSCC/Oropharynx, sinonasal	T1 N0 M0	Carboplatin, Paclitaxel	23	1
	17	M	70	HNSCC/Hypopharynx	T2 N2b M0	Carboplatin, Paclitaxel	16	3
	18	F	56	HNSCC/Oral Cavity	T4a N0 M0	Cisplatin	6	2
	19	M	50	HNSCC/Oral Cavity	T2 N2b M0	Cisplatin	2-14	1
	20	M	59	HNSCC/Oropharynx	rT4a N2b M0	Cisplatin or carboplatin	20	3
	21	M	80	HNSCC/Sinonasal Cavity	T4a N0 M0	Cisplatin	11	1
	22	F	55	HNSCC/Larynx	T4a N2b M0	Carboplatin, Paclitaxel	2	2
23	F	57	HNSCC/Oral Cavity	rT4 N0 M0	Cisplatin, Carboplatin, Paclitaxel	7	2	
24	M	58	HNSCC/Hypopharynx	T4a N2c M0	Cisplatin	12	2	
25	M	67	HNSCC/Oropharynx	T3 N1 M0	Cisplatin	21	3	
26	F	38	HNSCC/Oral Cavity	T1 N2b M0	Cisplatin	19	2	
27	M	75	HNSCC/Larynx	T3 N0 M0	Carboplatin, Paclitaxel	21	1	
28	M	67	HNSCC/Oropharynx	T1 N2b M0	Cisplatin	23	1	
29	M	80	HNSCC/Oral Cavity	rT2 N0 M0	Cisplatin or carboplatin	20	1	
30	F	42	HNSCC/Oropharynx	T2 N0 M0	Cisplatin	^b NED	1	
31	F	60	HNSCC/Oral Cavity	rT2 N0 M0	Cisplatin	33	1	
32	F	62	HNSCC/Oropharynx	T4a N0 M0	Carboplatin, Paclitaxel	35	1	
33	M	65	HNSCC/Sinonasal Cavity	T4a N0 M0	Cisplatin, Carboplatin, Paclitaxel	57	0	
34	M	47	HNSCC/Larynx	T1 N0 M0	Cisplatin	NED	3	
35	M	52	HNSCC/Oral Cavity	T2 N2b M0	Cisplatin or carboplatin	NED	1	
36	M	41	HNSCC/Oral Cavity	T4a N0 M0	Cisplatin, Ifosfamide, Paclitaxel	69	1	
37	M	58	HNSCC/Oropharynx	rT4 N0 M0	Carboplatin	29	2	
38	F	44	HNSCC/Oral Cavity	T1 N0 M0	Cisplatin or carboplatin	36	1	
39	M	64	HNSCC/Sinonasal Cavity	T1 N1 M0	Cisplatin	120	1	
40	F	34	HNSCC/Oral Cavity	T4a N0 M0	Carboplatin, Paclitaxel	67	1	
41	M	NA	HNSCC/Larynx	rT3 N0 M0	Cisplatin	32	2	
42	M	67	HNSCC/Oral Cavity	rT1 N1 M0	Carboplatin, Paclitaxel	26	1	
Sup Figure 8	Pair 1	M	41	HNSCC/Oral Cavity	T4a N0 M0	Cisplatin, Paclitaxel, Ifosfamide	60	^c 1/2
	Pair 2	M	58	HNSCC/Oropharynx	rT4 N0 M0	Carboplatin	29	1/1
	Pair 3	M	71	HNSCC/Oral Cavity	T2 N2b M0	Cisplatin	11	1/3
	Pair 4	F	38	HNSCC/Oral Cavity	T1 N2b M0	Cisplatin	19	1/2
	Pair 5	F	60	HNSCC/Oral Cavity	rT2 N0 M0	Cisplatin	33	0/1
	Pair 6	F	57	HNSCC/Oral Cavity	rT4 N0 M0	Cisplatin, Carboplatin, Paclitaxel	7	1/3
	Pair 7	M	NA	HNSCC/Larynx	rT3 N0 M0	Cisplatin	32	1/1
	Pair 8	M	61	HNSCC/Larynx	T4a N2b M0	Carboplatin	20	2/3
	Pair 9	M	80	HNSCC/Oral Cavity	rT2 N0 M0	Cisplatin or carboplatin	20	1/2
	Pair 10	M	75	HNSCC/Larynx	T3 N0 M0	Carboplatin, Paclitaxel	21	1/3
	Pair 11	F	56	HNSCC/Oral Cavity	T4a N0 M0	Cisplatin	6	1/2
	Pair 12	M	65	HNSCC/Sinonasal Cavity	T4a N0 M0	Cisplatin, carboplatin, Paclitaxel	57	0/1
	Pair 13	M	72	HNSCC/Oropharynx, Sinonasal	T1 N0 M0	Carboplatin, Paclitaxel	23	2/2

^aTime interval: time (months) between end of platinum-based chemotherapy (CT) treatment and tumor recurrence

^bNED: no evidence of disease

^cITPKB staining for paired tumors: Before CT/After CT

Supplemental Table 1. Clinical information for platinum-treated HNSCC patients whose tumors were examined for ITPKB expression.

	Cancer type	Sample #	Gender	Age	Diagnosis/subtype	Tumor stage	Treatment history prior to PDX	ITPKB level	Cisplatin IC ₅₀ (μM)
Figure 1C Sup Figure 1C	Head/neck	Pt 1	M	62	HNSCC/Oral Cavity	T4a N2c M0	Treatment naive	0.70	66.47
		Pt 2	M	69	HNSCC/Hypopharynx	T4a N2b M0	Treatment naive	0.66	50.39
		Pt 3	M	71	HNSCC/Oral Cavity	T4b N2b M0	Treatment naive	0.37	17.84
		Pt 4	M	71	HNSCC/Larynx	T4a N0 M0	Treatment naive	0.46	19.63
	Lung	Pt 5	M	72	Small cell lung carcinoma	Extensive stage	Cisplatin, etoposide, irinotecan	0.49	3.99
		^a Pt 6	F	60	Small cell lung carcinoma	Extensive stage	Carboplatin, etoposide	0.97	52.20
		Pt 7	M	71	Small cell lung carcinoma	Extensive stage	Cisplatin, etoposide	0.51	3.62
		Pt 8	M	50	Small cell lung carcinoma	Extensive stage	Cisplatin, etoposide	0.53	5.02
		Pt 9	M	76	Small cell lung carcinoma	Extensive stage	Carboplatin, etoposide	0.71	8.40
		Pt 10	F	56	Large cell neuroendocrine carcinoma	T3 N2 M1	Carboplatin, etoposide, Pemetrexed, Pembrolizumab Docetaxel	0.48	2.84
	Ovary	^b Pt 11	F	89	Papillary serous adenocarcinoma	FIGO III, pT3cN1	Treatment naive	0.72	28.53
		Pt 12	F	65	Ovarian serous adenocarcinoma	AJCC IV	Carboplatin, taxotere	0.42	6.66
		Pt 13	F	52	Ovarian Carcionsarcoma	AJCC IIIC	Treatment naive	0.65	33.60

^{a,b}PDX tumors used for *in vivo* xenograft study (Figure 8C-8F, Supplemental Figure 11)

Supplemental Table 2. Clinical information for HNSCC, lung, and ovarian cancer patient-derived xenograft tumors examined for ITPKB expression and cisplatin response.